J. Chem. Sci., Vol. 120, No. 1, January 2008, pp. 87–93.

Oximato bridged $Rh^{III}_2M^{II}$ and $Rh^{III}M^{I}$ species (M^{II} = Mn, Co, Ni; M^{I} = Cu, Ag)

INDRANIL BHATTACHARYYA, SANJIB GANGULY, BIKASH KUMAR PANDA and ANIMESH CHAKRAVORTY*

Department of Inorganic Chemistry, Indian Association for the Cultivation of Science, Kolkata 700 032
e-mail: animeshc31@yahoo.co.in

Abstract. The reaction of $[RhCl_2(HPhL)(PhL)]$ with $M^{II}(ClO_4)_2{\cdot}6H_2O$ in presence of alkali has furnished trinuclear $[RhCl_2(PhL)_2]_2M(H_2O)_2{\cdot}H_2O$ (HPhL is phenylazobenzaldoxime; M = Mn, Co, Ni). A similar reaction with $M^{I}(PPh_3)_2NO_3$ yielded binuclear $[RhCl_2(PhL)_2]M(PPh_3)_2$ (M = Cu, Ag). In these molecules the oximato group acts as a bridge between Rh^{III} (bonded at N) and M^{II} or M^{I} (bonded at O). In structurally characterized $[Rh^{III}Cl_2(PhL)_2]_2Mn(H_2O)_2.H_2O$ the centrosymmetric distorted octahedral MnO_6 coordination sphere is spanned by four oximato oxygen atoms and two water molecules lying in *trans* position. In the lattice the neighbouring molecules are held together by $H_2O{\cdots}H_2O{\cdots}H_2O$ hydrogen bonds generating infinite zigzag chains. The manganese atoms lie parallel to the C-axis, the shortest Mn…Mn distance being 7·992 Å. Magnetic exchange interactions if any are small as seen in room temperature magnetic moments. The manganese system displays a strong EPR signal near $g = 2{\cdot}00$. In the complex $[RhCl_2(PhL)_2]Cu(PPh_3)_2$ the copper atom is coordinated to two oximato oxygen atoms and the two phosphorus atoms in a distorted tetrahedral geometry. The softness of the phosphine ligand is believed to sustain the stable coordination of hard oximato oxygen to soft Cu^{I}. The coordination sphere of the Rh^{III} atom in both the complexes is uniformly *trans*-RhN_4Cl_2.

Keywords. Polynuclear complexes; oximato bridging; rhodium–manganese complexes; rhodium–copper complexes.

1. Introduction

Hetero-diatomic N, O-bridging of transition metal ions by the oximato function as in **1** has been known for long[1] and interest in the use of this tool as a strategy for designing interesting polynuclear species remains unabated.[2–10] The majority of this activity has generally concerned metal ions of the first transition series. Heavier ions occur in only a few scattered examples such as Pd_3[11], $PdCu_2$[12], Os_2M[13] and Os_3[14] species.

Rhodium(III) arylazooximates of type **2** abbreviated as $[RhCl_2(HArL)(ArL)]$ have been reported[15] from this laboratory (HArL is arylazobenzaldoxime). The *cis* disposition of the two oxime functions makes **2** a potential ligand for binding another metal ion via displacement of the bridge proton. In this work it is demonstrated that this indeed happens leading to novel binuclear and trinuclear species of types $Rh^{III}M^{I}$ (M = Cu, Ag) and $Rh^{III}_2M^{II}$ (M = Mn, Co, Ni) which have been isolated and characterized. Only the species with Ar = Ph are reported here.

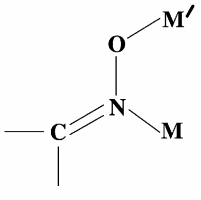

1

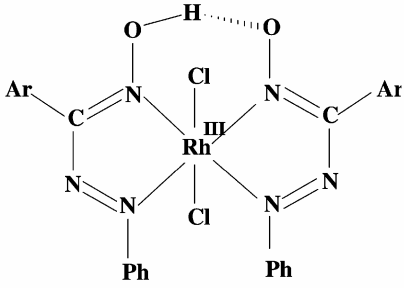

$RhCl_2(ArL)(HArL)$

2

2. Experimental

2.1 *Materials and methods*

The starting complexes $Cu^{I}(PPh_3)_2NO_3$[16], $Ag^{I}(PPh_3)_2NO_3$[17] and *trans*-$[Rh^{III}Cl_2(HPhL)(PhL)]$[15] were synthesized as reported. Hydrated transition metal perchlorates were prepared by treating the corresponding metal carbonates with 70% aqueous perchloric acid, followed by re-crystallization. All other chemicals and solvents were of reagent grade and were used as received. Electronic and IR spectra were recorded

*For correspondence

with a Shimadzu UV-1601 PC and Nicolet Magna IR series II/Perkin Elmer 783 spectrometers. Room temperature magnetic susceptibility was measured with a Model 155 PAR vibrating sample magnetometer fitted with a Walker Scientific L75FBAL magnet. Microanalysis (C, H, N) were performed using a Perkin-Elmer 240C elemental analyzer.

2.2 *Synthesis of the complexes*

2.2a *$[Rh^{III}Cl_2(PhL)_2]_2M^{II}(H_2O)_2.H_2O$*: These complexes were synthesized in good yields (70–80%) by reacting *trans*-$[Rh^{III}Cl_2(HPhL)(PhL)]$ and $M^{II}(ClO_4)_2\cdot 6H_2O$ in 2 : 1 molar ratio in presence of alkali . Details of a representative case (M = Mn) are given below. The other compounds (M = Co, Ni) were prepared analogously.

2.2b *$[RhCl_2(PhL)_2]_2Mn(H_2O)_2\cdot H_2O$:* To a suspension of *trans*-$[RhCl_2(HPhL)(PhL)]$ (0·2 g, 0·34 mmol) in 15 ml of absolute ethanol was added NaOH (0·014 g, 0·35 mmol) and the contents were stirred till dissolution. To the green solution thus obtained an ethanolic solution of $Mn^{II}(ClO_4)_2\cdot 6H_2O$ (0·062 g, 0·17 mmol) was added drop-wise. The colour changed to deep red and the contents were allowed to stir for 2 h. The dark red crystalline precipitate that separated was filtered, washed with ethanol and dried *in vacuo* over fused $CaCl_2$. Yield: 0·339 g, 75%. Anal Calc for $C_{52}H_{46}N_{12}O_7Cl_4Rh_2Mn$: C, 46·14; H, 3·42; N, 12·42%. Found: C, 46·4; H, 3·37; N, 12·48%. IR (KBr, cm^{-1}): 3400 (H_2O stretch), 360 (Rh–Cl stretch). UV-Vis (CH_2Cl_2, λ_{max}(nm) (ε, M^{-1} cm^{-1})): 575 (6850), 550 (5900), 460 (12000), 410 (16370), 360 (18030) μ_{eff} = 5·94 μB. EPR *g* values (polycrystalline): 2·014 (major); 1·542, 2·716, 4·628, 5·975 (minor).

2.2c *$[RhCl_2(PhL)_2]_2Co(H_2O)_2.H_2O$: Trans*-$[RhCl_2(HPhL)(PhL)]$ (0·2 g, 0·34 mmol), NaOH (0·014 g, 0·35 mmol) and $Co^{II}(ClO_4)_2\cdot 6H_2O$ (0·063 g, 0·17 mmol) were used. Yield: 0·348 g, 77%. Anal. Calc. for $C_{52}H_{46}N_{12}O_7Cl_4Rh_2Co$: C, 46·00; H, 3·41; N, 12·38%. Found: C, 46·08; H, 3·37; N, 12·37%. IR (KBr, cm^{-1}): 3400 (H_2O stretch), 360 (Co–Cl stretch). UV-Vis (CH_2Cl_2, λ_{max} (nm) (ε, M^{-1} cm^{-1})): 595 (7920), 585 (7600), 450 (15070), 410 (19700), 360(21500) μ_{eff} = 5·13 μB. EPR *g* values after doping with 1% $[RhCl_2(PhL)_2]_2Mn(H_2O)_2.H_2O$ (polycrystalline): 2.001 (major); 1·538, 2·650, 4·596, 5·868 (minor).

2.2d *$[RhCl_2(PhL)_2]_2Ni(H_2O)_2\cdot H_2O$: Trans*-$[RhCl_2(HPhL)(PhL)]$ (0·2 g, 0·32 mmol), NaOH (0·013 g, 0·33 mmol) and $Ni(ClO_4)_2\cdot 6H_2O$ (0·059 g, 0·16 mmol) were employed. Yield: 0·329 g, (73%). Anal. Calc. for $C_{52}H_{46}N_{12}O_7Cl_4Rh_2Ni$: C, 46·01; H, 3·42; N, 12·38%. Found: C, 46·09; H, 3·48; N, 12·34%. IR (KBr, cm^{-1}): 3400 (H_2O stretch), 355 (Co–Cl stretch). UV-Vis (CH_2Cl_2, λ_{max} (nm) (ε, M^{-1} cm^{-1})): 580 (7560), 560 (6740), 460 (10230), 415 (15330), 360(15970) μ_{eff} = 5·20 μB.

EPR *g* values after doping with 1% $[RhCl_2(PhL)_2]_2Mn(H_2O)_2.H_2O$ (polycrystalline): 1.983 (major); 1·660, 2·416, 3·043, 3·774, 4·668, 6·262 (minor)

2.2e *$[Rh^{III}Cl_2(PhL)_2]M^{I}(PPh_3)_2$ (M = Cu, Ag):* The $[Rh^{III}Cl_2(PhL)_2]M^{I}(PPh_3)_2$ complexes were synthesized in good yields by reacting *trans*-$[Rh^{III}Cl_2(HPhL)(PhL)]$ in ethanol with equimolar amount of $M^{I}(PPh_3)_2NO_3$ in presence of base. Details of a representative case (M = Cu) are given below.

2.2f *$[RhCl_2(PhL)_2]Cu(PPh_3)_2$:* To a suspension of *trans*-$[RhCl_2(HPhL)(PhL)]$ (0·2 g, 0·34 mmol) in 15 ml of absolute ethanol was added NaOH (0·014 g, 0·35 mmol) and the contents were stirred till dissolution. An ethanolic solution of $Cu(PPh_3)_2NO_3$ (0·222 g, 0·34 mmol) was then added and the mixture was stirred for 5 h affording a blue-green crystalline precipitate which was collected by filtration and washed with 50% aqueous ethanol followed by drying in vacuo. Yield: 0·324 g, (79%). Anal. Calc. for $C_{62}H_{50}N_6O_2Cl_2P_2CuRh$: C, 61·52; H, 4·16; N, 6·94%. Found: C, 61·46; H, 4·14; N, 6·99%. IR (KBr, cm^{-1}): 360 (Rh–Cl stretch). UV-Vis (CH_2Cl_2, λ_{max} (nm) (ε, M^{-1} cm^{-1}): 610 (2870), 450 (4330), 400 (5330).

2.2g *$[RhCl_2(PhL)_2]Ag(PPh_3)_2$: Trans*-$[RhCl_2(HPhL)(PhL)]$ (0·2 g, 0·34 mmol), NaOH (0·014 g, 0·35 mmol) and $Ag(PPh_3)_2NO_3$ (0·236 g, 0·34 mmol) were employed. Yield: 0·311 g, (73%). Anal. Calc. for $C_{62}H_{50}N_6O_2Cl_2P_2AgRh$: C, 59·35; H, 4·02; N, 6·70%. Found: C, 59·42; H, 4·05; N, 6·62%. IR (KBr, cm^{-1}): 365 (Rh–Cl stretch). UV-Vis (CH_2Cl_2, λ_{max} (nm) (ε, M^{-1} cm^{-1})): 590 (2550), 460 (4300), 415 (7600).

2.3 *X-ray crystallography*

Single crystals of $[RhCl_2(PhL)_2]_2Mn(H_2O)_2.H_2O.CH_2Cl_2$ and $[RhCl_2(PhL)_2]Cu(PPh_3)_2$ were grown by slow diffusion of hexane into dichloromethane solution at room temperature. Cell parameters were de-

termined by least squares fit of 30 machine-centered reflections (2θ range 14–28°) on a Siemens *R*3*m*/*v* four-circle diffractometer with a graphite-monochromated Mo–Kα radiation (λ = 0·71073). Two check reflections measured after every 198 reflections showed no significant intensity reduction. All data were corrected for Lorentz polarization effects and an empirical absorption correction[18] was performed on the basis of an azimuthal scan of six reflections for each crystal. The metal atoms were located from Patterson maps, and the rest of the non-hydrogen atoms emerged from successive Fourier synthesis. The structures were refined by a full-matrix least squares procedure. All non-hydrogen atoms were refined anisotropically and hydrogen atoms added at calculated positions. Calculations were performed using the SHELXTL, version 5.03[19] program package. Significant crystal data are listed in table 3.

3. Results and discussion

3.1 *Synthesis and characterization*

Reaction of $[RhCl_2(PhL)_2]^-$ (via deprotonation of **2** (Ar = Ph)) with $M(ClO_4)_2{\cdot}6H_2O$ (M = Mn, Co, Ni) in ethanol in molar ratio 2 : 1 has furnished the dark red complexes of type $[RhCl_2(PhL)_2]_2M(H_2O)_2$, **3**. On the other hand, its reaction with $M(PPh_3)_2(NO_3)$ (M = Cu, Ag) in molar ratio 1 : 1 yielded the bluish-green complex of type $[RhCl_2(PhL)_2]M(PPh_3)_2$, **4**.

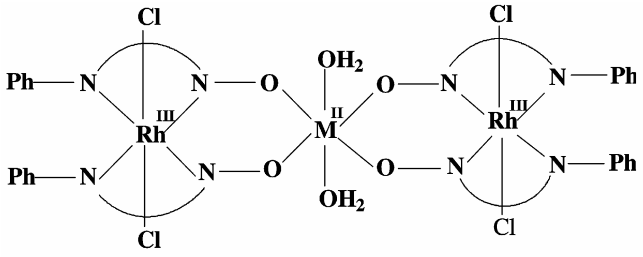

3

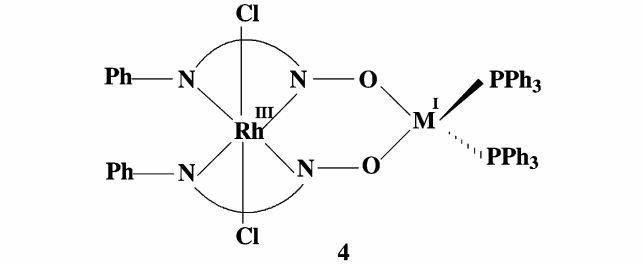

4

Selected characterization data are given in the experimental section. The complexes uniformly display an Rh–Cl stretch in the region 350–360 cm^{-1}. The type **3** species display a broad and strong H_2O vibration near 3400 cm^{-1}. In dichloromethane **3** and **4** richly absorb in the 350–700 nm region. While the type **4** species are diamagnetic, the polycrystalline type **3** complexes have room temperature magnetic moments of 5·94 μB (M = Mn), 5·13 μB (M = Co) and 3·21 μB (M = Ni) corresponding to high-spin d^5, d^7 and d^8 states respectively. In the structure of $[RhCl_2(PhL)_2]_2Mn(H_2O)_2$ the minimum manganese–manganese distance is 7·992 Å (*vide infra*) and intermanganese interaction if any is small. The M = Ni and Co complexes are EPR silent presumably due to relaxation effects.[20] The manganese complex is EPR-active and in the polycrystalline phase (298 K) the major signal occur near g = 2. In addition a number of minor signals arising out of zero field splitting[21] in the distorted octahedral geometry are observed (g-range 1·5–6·0). In frozen dichloromethane–toluene glass (77 K), ^{55}Mn hyperfine splittings (A ~ 100G) are clearly resolved specially in the major line. The manganese complex grows freely in the lattice of the corresponding nickel and cobalt species suggesting that they are isostructural. The doped species display EPR spectra closely analogous to that of the manganese complex.

3.2 *Structure*

3.2a *$[RhCl_2(PhL)_2]_2Mn(H_2O)_2.H_2O.CH_2Cl_2$:* The lattice consists of two metrically similar but crystallographically distinct centrosymmetric (inversion center at Mn) trinuclear molecules (molecule 1 and molecule 2) each of composition $[RhCl_2(PhL)_2]_2Mn(H_2O)_2$. The remaining water molecule links molecule 1 and molecule 2 (see below). A view of molecule 1 is depicted in figure 1 and selected bond parameters for both molecules are listed in table 1. The dichloromethane molecule occupies a general position and displays no unusual non-bonded interactions. The manganese atom has essentially displaced the oxime proton of two molecules of the parent complex **2** (Ar = Ph) making four oximato oxygen atoms available for equatorial coordination. The two axial positions of the distorted octahedral coordination sphere are occupied by water molecules.

The geometry of the RhN_4Cl_2 moiety and bond lengths therein are essentially similar to those in **2** (Ar = Ph).[15] The five-membered chelate rings are satisfactorily planar but the six-membered ring in-

Table 1. Selected bond lengths and angles [Å, °] for $[RhCl_2(PhL)_2]_2Mn(H_2O)_2.H_2O{\cdot}CH_2Cl_2$ **3**.

Molecule 1		Molecule 2	
Mn(1)–O(1)	2·159(4)	Mn(2)–O(4)	2·120(4)
Mn(1)–O(2)	2·124(4)	Mn(2)–O(5)	2·124(4)
Mn(1)–O(3)	2·136(5)	Mn(2)–O(6)	2·169(5)
Rh(1)–N(1)	2·053(5)	Rh(2)–N(7)	2·054(5)
Rh(1)–N(3)	2·010(5)	Rh(2)–N(9)	2·023(5)
Rh(1)–N(6)	2·015(5)	Rh(2)–N(12)	2·016(5)
Rh(1)–N(4)	2·048(5)	Rh(2)–N(10)	2·055(5)
Rh(1)–Cl(1)	2·332(2)	Rh(2)–Cl(3)	2·329(2)
Rh(1)–Cl(2)	2·320(2)	Rh(2)–Cl(4)	2·333(2)
N(1)–N(2)	1·273(6)	N(7)–N(8)	1·260(6)
N(3)–O(1)	1·283(6)	N(12)–O(5)	1·278(6)
N(6)–O(2)	1·286(6)	N(9)–O(4)	1·284(6)
O(3)···O(7)	2·796(5)	O(6)···O(7)	2·855(5)
O(2)–Mn(1)–O(3A)	87·8(2)	O(4A)–Mn(2)–O(6)	93·1(1)
O(2)–Mn(1)–O(3)	92·2(2)	O(5)–Mn(2)–O(6)	88·5(2)
O(2A)–Mn(1)–O(1)	95·0(2)	O(5A)–Mn(2)–O(4)	93·0(2)
O(2)–Mn(1)–O(1)	85·0(2)	O(6)–Mn(2)–O(4)	86·9(2)
O(3A)–Mn(1)–O(1)	85·7(2)	O(6A)–Mn(2)–O(4)	93·1(2)
O(3)–Mn(1)–O(1)	94·3(2)	O(5)–Mn(2)–O(4)	87·0(2)
N(3)–Rh(1)–N(6)	100·4(2)	N(9)–Rh(2)–N(12)	100·8(2)
N(6)–Rh(1)–N(4)	75·6(2)	N(9)–Rh(2)–N(10)	176·5(2)
N(3)–Rh(1)–N(1)	75·9(2)	N(9)–Rh(2)–N(7)	75·8(2)
O(1)–N(3)–Rh(1)	125·5(3)	O(4)–N(9)–Rh(2)	125·4(3)
O(2)–N(6)–Rh(1)	123·9(3)	O(5)–N(12)–Rh(2)	125·0(3)
N(4)–Rh(1)–N(1)	108·1(2)	N(12)–Rh(2)–N(10)	75·7(2)
Cl(1)–Rh(1)–Cl(2)	177·49(6)	Cl(3)–Rh(2)–Cl(4)	178·81(6)
O(3)···O(7)···O(6)	134·4(2)	O(7)···O(6)–Mn(2)	111·9(2)

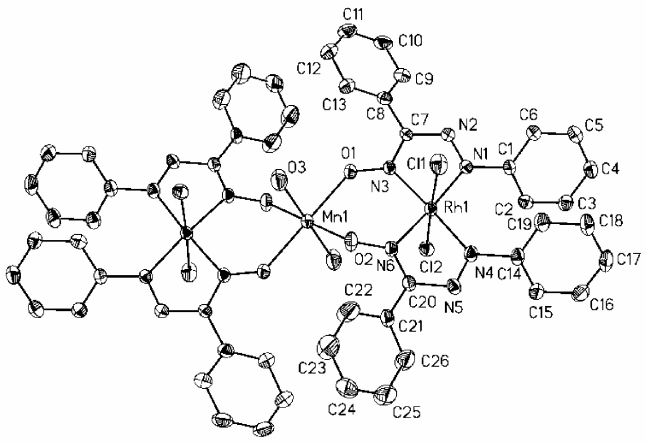

Figure 1. ORTEP plot (30% probability ellipsoids) and atom labelling scheme for $[Rh^{III}Cl_2(PhL)_2]_2Mn(H_2O)_2{\cdot}H_2O{\cdot}CH_2Cl_2$.

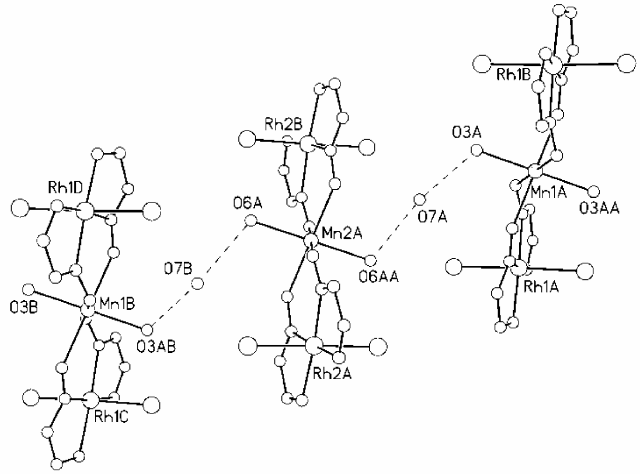

Figure 2. Perspective view of $[Rh^{III}Cl_2(PhL)_2]_2Mn(H_2O)_2{\cdot}H_2O{\cdot}CH_2Cl_2$ in the lattice showing the intermolecular zigzag chain.

corporating both rhodium and manganese lacks planarity due to a relatively large (0·81 Å in molecule 1 and 0·68 Å in molecule 2) deviation of the manganese atom from RhN_2O_2 plane (mean deviation 0·05 Å).

The average Rh–N^o distance is 0·04 Å shorter than the Rh–N^a distance (N^o and N^a are respectively oxime and azo nitrogen atoms).[15] Corresponding to oxime deprotonation, the N–O length shortens in going from **2** (Ar = Ph) (average, 1·32 Å) to the pre-

Table 2. Selected bond lengths and angles [Å, °] for $[RhCl_2(PhL)_2]Cu(PPh_3)_2$ **4**.

Rh–N(6)	2·007(5)	N(1)–N(2)	1·281(8)
Rh–N(4)	2·036(5)	Rh–N(3)	2·015(5)
Rh–N(1)	2·046(6)	Rh–Cl(2)	2·327(2)
Cu–O(2)	2·060(5)	Rh–Cl(1)	2·334(2)
Cu–O(1)	2·067(4)	N(3)–O(1)	1·278(7)
Cu–P(1)	2·283(3)	N(6)–O(2)	1·280(7)
Cu–P(1)	2·229(2)	N(4)–N(5)	1·276(8)
N(6)–Rh–N(3)	100·9(2)	N(6)–Rh–N(4)	76·2(2)
N(3)–Rh–N(4)	176·2(2)	N(4)–Rh–N(1)	107·0(2)
N(3)–Rh–N(1)	76·0(2)	Cl(1)–Rh–Cl(2)	177·88(7)
N(6)–Rh–N(1)	176·7(2)		

Table 3. Technical details of data acquisition and selected refinement results for **3** and **4**.

Compound	$[RhCl_2(PhL)_2]_2Mn(H_2O)_2\cdot H_2O\cdot CH_2Cl_2$ **3**	$[RhCl_2(PhL)_2]Cu(PPh_3)_2$ **4**
Empirical formula	$C_{53}H_{48}Cl_6MnN_{12}O_7Rh_2$	$C_{62}H_{50}Cl_2CuN_6O_2P_2Rh$
Formula weight	1438·49	1210·37
Temperature (K)	293	293
Wavelength	0·71073	0·71073
Crystal system	Triclinic	Triclinic
Space group	P–1	P–1
a (Å)	12·808(3)	13·147(7)
b (Å)	15·290(3)	13·568(5)
c (Å)	15·984(3)	19·537(9)
α (°)	106·06(3)	74·09(3)
β (°)	94·80(3)	81·68(4)
γ (°)	102·66(3)	68·06(4)
Volume ($Å^3$)	2899·9	3105
Z	2	2
μ [mm^{-1}]	1·115	0·790
F(000)	1446	1236
Crystal size (mm^3)	0·44 × 0·38 × 0·14	0·40 × 0·35 × 0·20
D_{calcd} (Mg/m^3)	1·647	1·294
hkl range	0/13, –16/16, –17/17	0/14, –13/14, –20/21
2θ range (°)	1·64–23·55	1·67–23·55
Reflections collected	7745	8292
Reflections unique	7618	8131
Data ($Fo > 2\sigma(Fo)$)	7598	8091
Parameters	733	685
R_{int}	0·0610	0·0572
$R1[Fo > 2\sigma(Fo)]$	0·0435	0·0622
*WR*2 for all unique data	0·1336	0·2333
Goodness of fit	1·045	1·067

sent complex (average, 1·28 Å). There is a corresponding increase in the O···O distance from 2·51 Å to 2·90 Å associated with the increase of the N°–Rh–N° and Rh–N°–O angles from 98° to 100° and 121° to 125° respectively.

Molecule 1 and molecule 2 are interlinked via an interesting form of H_2O…H_2O…H_2O hydrogen bonding as depicted in figure 2. In effect a water trimer is acting as a bridging bidentate ligand between two manganese atoms. In the zigzag chain thus produced the manganese atoms lie parallel to the crystallographic C-axis, the shortest Mn…Mn distance being 7·992(1)Å which corresponds to $c/2$. This large distance is consistent with the room temperature magnetic moment lying near the normal s = 5/2 value.

3.2b *$[RhCl_2(PhL)_2]Cu(PPh_3)_2$:* The lattice consists of only one type of molecules. A molecular view is

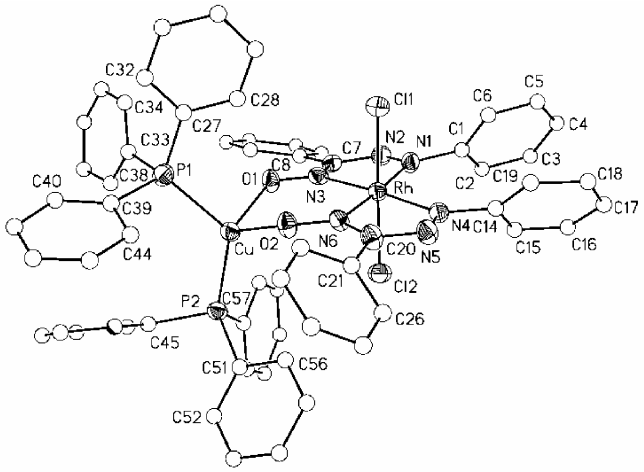

Figure 3. ORTEP plot (30% probability ellipsoids) and atom labelling scheme for $[RhCl_2(PhL)_2]Cu(PPh_3)_2$. For clarity the phenyl rings are isotropically depicted.

shown in figure 3 and selected bond parameters are listed in table 3. The CuP_2 fragment is chelated by two oximato oxygen atoms generating a highly distorted tetrahedral CuO_2P_2 configuration in which the angles at the metal site span the range 90·9° (O1–Cu–O2) to 124·5° (P1–Cu–P2). The oximato oxygen atom is a hard donor and its stable coordination to soft Cu^I is sustained by the soft nature of the phosphine ligands. As in the manganese complex the five-membered chelate rings are satisfactorily planar and the six-membered ring is non-planar. In the latter the copper atom lie 0·6 Å away from the plane of RhN_2O_2 fragment. The geometry and dimensions of the RhN_4Cl_2 sphere are closely similar to those in manganese complex.

The structure of the iron(II)–copper(I) complex $[Fe(PhL)_3]Cu(PPh_3)$ having $CuO^o{}_3P$ coordination sphere is known.[22] The average Cu–P (2·26 Å) and Cu–O (2·07 Å) distances in $[RhCl_2(PhL)_2]Cu(PPh_3)_2$ are respectively larger and smaller than those (2·15 Å and 2·10 Å) in $[Fe(PhL)_3]Cu(PPh_3)$. To our knowledge these are the only two structurally characterized binuclear complexes incorporating oximato oxygen coordination to Cu^I.

4. Conclusion

In this work the first examples of oximato bridged hetero-binuclear and hetero-trinuclear species incorporating the $Rh^{III}M^I$ (M = Cu, Ag) and $Rh_2{}^{III}M^I$ (M = Mn, Co, Ni) cores have been successfully assembled. In the structure of $[RhCl_2(PhL)_2]_2Mn(H_2O)_2{\cdot}H_2O{\cdot}CH_2Cl_2$ a hydrogen bonded water trimer acts as bridging ligand between two metrically similar but crystallographically distinct molecules each having a centrosymmetric pseudooctahedral MnO_6 coordination sphere. The complex $[RhCl_2(PhL)_2]Cu(PPh_3)_2$ incorporating a highly distorted tetrahedral coordination sphere represents a rare example of the sustenance of soft Cu^I by hard oximato oxygen in the presence of soft tertiary phosphine coligand.

Supplementary material

Crystallographic data (excluding structure factors) for the structural analysis reported in this paper have been deposited with the The Cambridge Crystallographic Data Centre as supplementary publication no. CCDC 668942 & CCDC 668943 corresponding to $[Rh^{III}Cl_2(PhL)_2]_2Mn(H_2O)_2{\cdot}H_2O{\cdot}CH_2Cl_2$ **3** and $[Rh^{III}Cl_2(PhL)_2]Cu^I(PPh_3)_2$ **4**. Copies of the data can be obtained via www.ccdc.cam.ac.uk/data_request/cif, or by emailing data_request@ccdc.cam.ac.uk, or by contacting CCDC, 12, Union Road, Cambridge CB2 1 EZ, UK (fax: +44 1223-336033).

Acknowledgement

We thank the Department of Science and Technology (DST) and Council of Scientific and Industrial Research (CSIR) for financial support.

References

1. Chakravorty A 1974 *Coord. Chem. Rev.* **13** 1
2. Mannivannan V, Dutta S, Basu P and Chakravorty A 1993 *Inorg. Chem.* **32** 4807
3. Costes J-P, Dahan F and Dupuis A 2000 *Inorg. Chem.* **39** 5994
4. Fukita N, Ohaba M, Shiga T, Okawa H and Ajiro Y 2001 *J. Chem. Soc., Dalton Trans.* 64
5. Chaudhuri P 2003 *Coord. Chem. Rev.* **243** 143
6. Jiang Y-B, Kou H-Z, Wang R-J, Cui A-L and Ribas J 2005 *Inorg. Chem.* **44** 709
7. Weyhermüller T, Wagner R, Khanra S and Chaudhuri P 2005 *J. Chem. Soc., Dalton Trans.* 2539
8. Fritsky I O, Kozlowski H, Kanderal O M, Haukka M, Kozlowska-Swiatek J, Gumienna-Kontecka E and Meyer F 2006 *Chem. Commun.* 4125
9. Milios C J, Stamatatos T C and Perlepes S P 2006 *Polyhedron* **25** 134
10. Afrati T, Zaleski C M, Dendrinou-Sammara C, Mezei G, Kampf J W, Pecoraro V L and Kessissoglou D P 2007 *J. Chem. Soc. Dalton Trans.* 2658

11. Mawby A and Pringle G E 1971 *Inorg. Nucl. Chem.* **33** 1989
12. Chaudhuri P, Winter M, Della Vedova B P C, Bill E, Trautwein A, Gehring S, Fleischauer P, Nuber B and Weiss J 1991 *Inorg. Chem.* **30** 2148
13. Ghosh B K, Mukherjee R N and Chakravorty A 1987 *Inorg. Chem.* **26** 1946
14. Chao M-H, Kumaresan S, Wen Y-S, Lin S-C, Hwu J R and Lu K-L 2000 *Organometallics* **19** 714
15. Ganguly S, Mannivannan V and Chakravorty A 1998 *J. Chem. Soc. Dalton Trans.* 461
16. Gysling H J 1979 *Inorg. Synth.* **19** 92
17. Barron P F, Dyason J C, Healy P C, Engelhardt L M, Skelton B W and White A H 1986 *J. Chem. Soc. Dalton Trans.* 1965
18. North A C T, Philips D C and Mathews F A 1968 *Acta Crystallogr.* **A24** 351
19. Sheldrick G. M, SHELXTL, Version 5.03, 1999 Siemens Analytical X-ray system, Madison, WI
20. Pal S, Mukherjee R N, Tomas M, Falvello L R and Chakravorty A 1986 *Inorg. Chem.* **25** 200
21. Chakraborty P, Chandra S K and Chakravorty A 1993 *Inorg. Chem*. **32** 5349
22. Mannivannan V, Dutta S, Basu P and Chakravorty A 1993 *Inorg. Chem*. **32** 4807